A New Class of Alkaloids from a Dendrobatid Poison Frog: A Structure for Alkaloid 251F

T. F. Spande, H. M. Garraffo, H. J. C. Yeh,
Q.-L. Pu, L. K. Pannell, and J. W. Daly

J. Nat. Prod., **1992**, 55 (6), 707-722• DOI:
10.1021/np50084a002 • Publication Date (Web): 01 July 2004

Journal of Natural Products
Vol. 55, No. 6, pp. 707-722, June 1992

A NEW CLASS OF ALKALOIDS FROM A DENDROBATID POISON FROG: A STRUCTURE FOR ALKALOID **251F**

T.F. SPANDE, H.M. GARRAFFO, H.J.C. YEH, Q.-L. PU, L.K. PANNELL, and J.W. DALY*

Laboratories of Bioorganic Chemistry and Analytical Chemistry, Bldg. 8, Room 1A17, National Institute of Diabetes, and Digestive and Kidney Diseases, National Institutes of Health, Bethesda, Maryland 20892

ABSTRACT.—Alkaloids of a new class are present in skin extracts of the dendrobatid poison frog, *Minyobates bombetes*, of Colombia. The structure of the major alkaloid of this class, **251F**, has been determined as a trimethylcyclopenta[*b*]quinolizidinemethanol **1** by nmr, gc-Ft-ir, and ms studies including ms-ms. At least nine congeners of **251F** were detected in these extracts.

Amphibians produce a wide variety of biologically active substances including alkaloids (1). The alkaloids are toxic or noxious and are presumed to be elaborated as a chemical defense against predators. Frogs from four genera of the family Dendrobatidae produce the widest variety of alkaloids, the so-called dendrobatid alkaloids, which have been classified as batrachotoxins, histrionicotoxins, gephyrotoxins, the pumiliotoxin-A class, 2,5-disubstituted decahydroquinolines, 3,5- and 5,8-disubstituted indolizidines, and the recently defined 1,4-disubstituted quinolizidines. Only a few of the dendrobatid alkaloids have been detected in other anurans (2,3).

Because of the large number of dendrobatid alkaloids detected (more than 200 alkaloids characterized during analysis of nearly fifty species of dendrobatid frogs) a code for the individual alkaloids was introduced in 1978 (4). This code employs the alkaloid's mol wt in boldface with an added letter to distinguish alkaloids with the same mol wt. In some cases where it appeared initially that an alkaloid might be an inseparable mixture of isomers, two letters and the mol wt were used. Several, e.g., **223AB**, **239AB**, **239CD**, have since been shown to be a single component. Due to the increasing number of isomers now being detected, prefixes (such as cis, trans, epi, etc.) and primes (A′, A″) have been introduced.

Recently, a group of eight miniature dendrobatid frog species have been placed in the genus *Minyobates* (5). One, the Colombian frog *Minyobates bombetes* Myers & Daly, contains an unusual dendrobatid alkaloid, **251F** (6), almost uniquely limited to this species (1). It is accompanied by two apparently related trace alkaloids, **249** and **265B**. At least thirty other alkaloids also were detected (6), some recognized as previously characterized alkaloids, such as **251D** and **267A** of the pumiliotoxin-A class, while others now are known to be 5,8-dialkylindolizidines or 1,4-dialkylquinolizidines. Further trace alkaloids that have been detected with capillary gc (Figure 1) appear related to **251F**, in having significant odd mass fragments. We group **251F** and at least nine congeners in a new dendrobatid alkaloid class with a cyclopenta[*b*]quinolizidine structure. The present paper reports evidence for a structure **1** for **251F**. The nomenclature accepted by *Chemical Abstracts* for **251F** would be a dodecahydro-3,7,10-trimethyl-2-hydroxymethylcyclopenta[*b*]quinolizidine. The parent ring system has only one entry: *Angew. Chem.*, **89**, 758 (1977). Instead of the *Chem. Abstr.* numbering, we have chosen a system which reflects a relationship with quinolizidines.

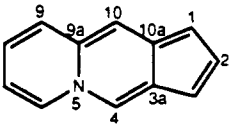

cyclopenta[*b*]quinolizine

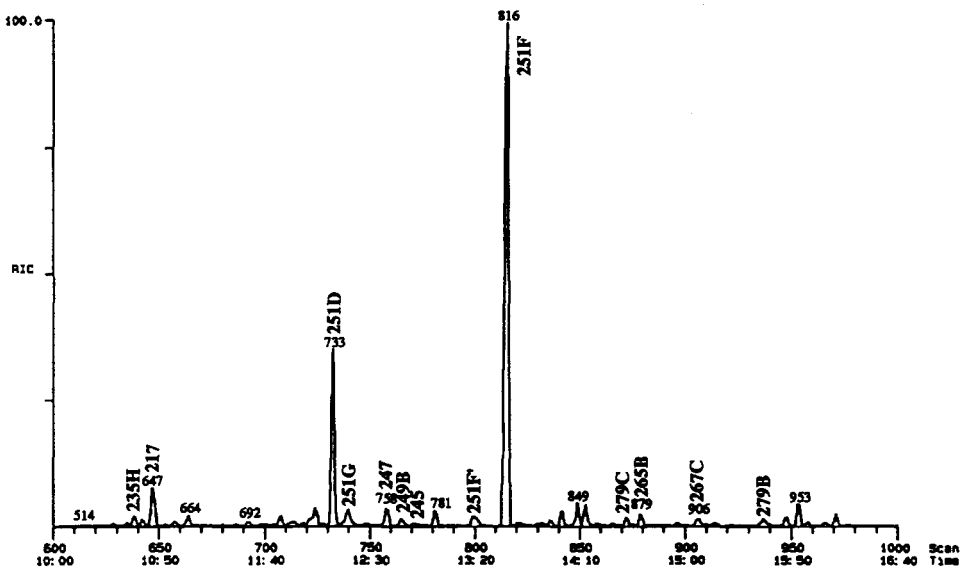

FIGURE 1. Gc-ms chromatogram of alkaloid fraction from skin extract of the poison frog *Minyobates bombetes*. A bonded fused silica OV-1 gc capillary column (25 m × 0.20 mm) programmed 100°–280° (10°/min) was used with a Finnigan Model 4500 mass spectrometer and INCOS data system. The mass range *m/z* 50 to 450 was scanned once a second to generate the X-axis scan numbers. All indicated alkaloids are **251F** congeners except the indolizidine **217** and pumiliotoxins **251D** and **267C**.

RESULTS AND DISCUSSION

The molecular ion of *m/z* 251 was confirmed for the major gc peak in the extract from *M. bombetes*. Cims with NH_3 gave a 1:1 ratio of ions at *m/z* 250 and 252, while isobutane gave the same ions in a 1:10 ratio and a weak ion at *m/z* 234 $[M+H-H_2O]^+$. The *m/z* 250 ion reflects the easy loss of H_2 from the protonated molecular ion, particularly with NH_3 cims. Deuteroammonia cims gave a 1:1 ratio of ions at *m/z* 251 and 254, the former resulting from a loss of HD from the deuteronated molecular ion, which has undergone one exchange.

Thermospray ms revealed *m/z* 252 for the major *M. bombetes* alkaloid on direct injection of the extract; this changed to *m/z* 254 when the sample was injected in a D_2O-containing buffer, again indicating one exchangeable hydrogen.

Upon hydrogenation of the extract, no change in retention time or mass spectrum was observed for **251F**, while acetylation converted it to a new material of longer retention time, with a mol wt of 293. This monoacetate showed no exchangeable hydrogen with deuteroammonia cims and gave fragment losses of 43, 59, and 73 in eims, the latter producing a 220 base peak, indicating a CH_2OAc group. Thus, **251F** is a tertiary amine with a primary alcohol, three rings, and no double bonds. The molecular formula, $C_{16}H_{29}NO$, was established by hrms as well as formulae for all significant ms peaks (Table 1).

Silica gel chromatography provided roughly 0.3 mg of **251F**, homogeneous by gc-ms. Eims fragmentation pathways, either proved or inferred, were analyzed using a Finnigan ion trap mass spectrometer especially configured for ms-ms studies (see Experimental) and are shown in Figure 2. At later stages of structure determination, these data were useful in screening hypotheses. Initially, however, we could only reach a few conclusions: (a) The major fragment, *m/z* 111, an uncommon odd-mass fragment,

TABLE 1. High Resolution Ms Analysis of **251F**.

m/z	% Total[a]	Formula	Loss from $[M]^+$
251[b]	54	$C_{16}H_{29}NO$	
250[b]	65	$C_{16}H_{28}NO$	H
236[b]	27	$C_{15}H_{26}NO$	CH_3
234[b]	5	$C_{16}H_{28}N$	OH
222[b]	28	$C_{14}H_{24}NO$	C_2H_5
221	30	$C_{15}H_{27}N$	CH_2O
220[b]	68	$C_{15}H_{26}N$	CH_3O
208[b]	7	$C_{13}H_{22}NO$	C_3H_7
195	17	$C_{12}H_{21}NO$	C_4H_8
194[b]	62	$C_{12}H_{20}NO$	C_4H_9
192[b]	12	$C_{13}H_{22}N$	C_3H_7O
181[b]	7	$C_{11}H_{19}N$	$C_5H_{10}O$
		$C_{10}H_{16}NO$	C_6H_{13}
166	12	$C_{11}H_{20}N$	C_5H_9O
164[b]	19	$C_{11}H_{18}N$	$C_5H_{11}O$
152[b]	35	$C_{10}H_{18}N$	$C_6H_{11}O$
150[b]	17	$C_{10}H_{16}N$	$C_6H_{13}O$
140	8	$C_9H_{18}N$	
138[b]	8	$C_9H_{16}N$	
136	9	$C_9H_{14}N$	
124[b]	8	$C_8H_{14}N$	
122[b]	4	$C_8H_{12}N$	
112	43	$C_7H_{14}N$	
111[b]	100	$C_7H_{13}N$	
98[b]	35	$C_6H_{12}N$	
96	17	$C_6H_{10}N$	
82	15	C_5H_8N	

[a]Measured with the Finnigan Model 4500 mass spectrometer in electron impact mode (70 eV).

[b]We thank Dr. Peter Roller, NCI, NIH for these exact masses measured with the photoplate technique. These and the remaining masses were also measured at the Mass Spectrometry Laboratory, Ed Larker, Director, University of Minnesota. All measured masses were within ± 3.1 mmu of the calculated mass.

arises from *m/z* 221 and not by any direct process from $[M]^+$. (b) The butyl loss can occur directly (*m/z* 251↦194) or in two steps (−H, $-C_4H_8$; *m/z* 251↦250↦194) and at two points in the pathway (*m/z* 221↦164). (c) The *m/z* 152 ion, which is a significant oxygen-free fragment and a major ion in one **251F** congener (see Table 2), probably arises directly from the parent ion.

A gc-Ft-ir spectrum of **251F** (Figure 3) revealed a ν_{OH} absorption at 3666 cm^{-1}, as expected for a primary, non-hydrogen-bonded alcohol, and a significant Bohlmann band pattern at 2800–2650 cm^{-1} reminiscent of that of some quinolizidines. In fact, not only did 1,7-dimethylquinolizidine [**2**] (7) exhibit similar Bohlmann bands (Figure 3), it also had many points of similarity with **251F** in its mass spectrum, viz., a large $[M-H]^+$ peak, a significant $[M-Me]^+$ peak (even though neither Me substituent is at a carbon adjacent to nitrogen), a large loss of C_4H_9, and, most importantly, a base peak at *m/z* 111. Ms-ms studies on this sample (see Figure 2) indicated some pathways common to **251F** (e.g., *m/z* 111↦96, 82); however, the butyl cleavage is seen as a loss of hydrogen and two ethylene cleavages in addition to hydrogen and C_4H_8, and 42 amu losses were more significant for **2** than for **251F**. In addition, the *m/z* 111 fragment can

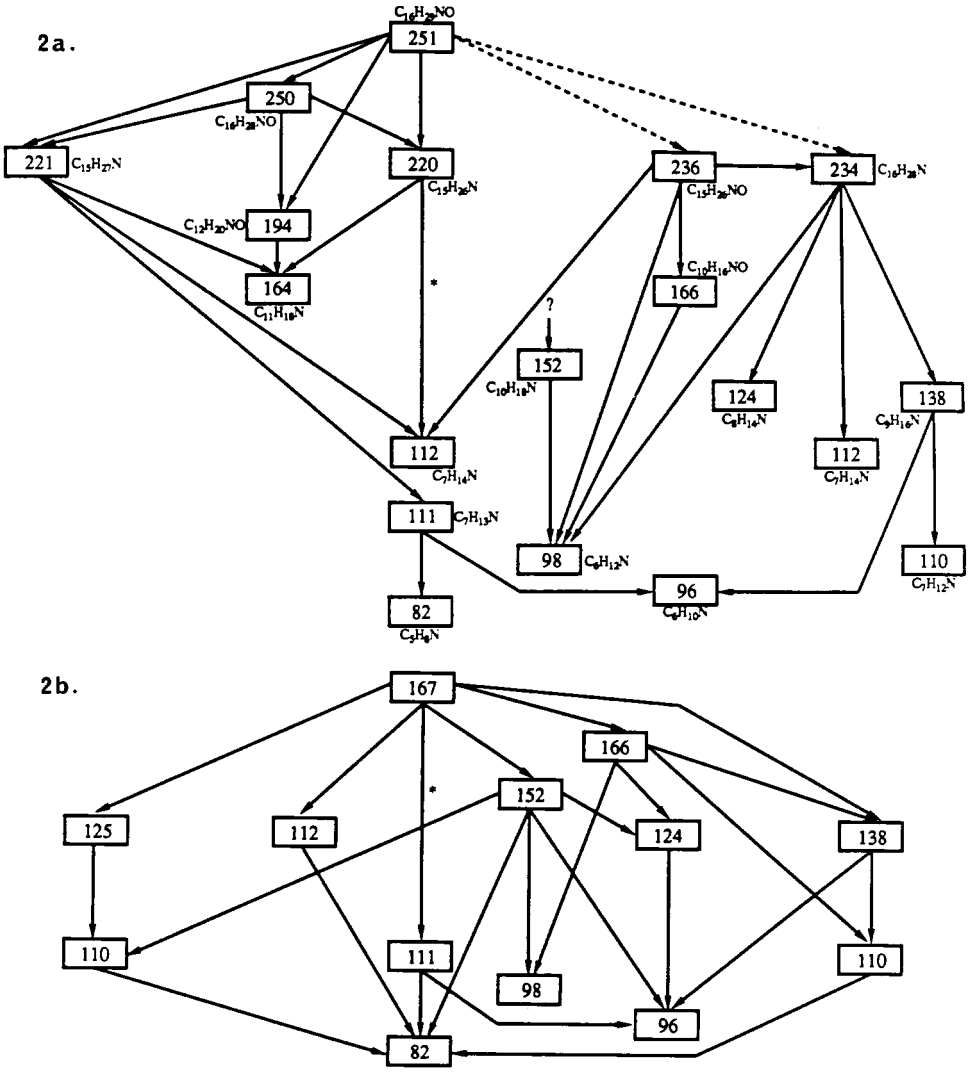

FIGURE 2. Analysis of pathways for ms-ms fragmentation for (a) alkaloid **251F** [**1**] and (b) 1,7-dimethylquinolizidine [**2**]. Proven pathways are shown by solid lines, while inferred pathways are shown by dashed lines. Major pathways are indicated by an asterisk.

evidently occur directly from $[M]^+$ in **2**. This probably does not reflect any essential difference with **251F**, since the latter may simply have a very facile $[M-30]^+$ cleavage preceding that yielding the *m/z* 111 fragment. Despite some ms-ms differences, it appeared likely that **251F** contained a methylquinolizidine moiety. It is notable also that several of the trace alkaloids accompanying **251F** were recognized as 1,4-dialkylquinolizidines by characteristic *m/z* 110 and 84 eims fragments and Ft-ir Bohlmann band patterns.

A sample of **251F** (0.34 mg) in D_2O containing 5 μmol DCl provided a 500 MHz ^{1}H-nmr spectrum (Figure 4a) in which 21 out of its 29 protons could be discerned and most of the important couplings measured. A 2D H-COSY spectrum (Table 4) clarified many couplings; these were corroborated and extended by 1D decoupling experiments. The ^{1}H-nmr data of Tables 3 and 4 with computer modelling studies and ^{13}C-nmr and

TABLE 2. Ms Data on Congeners of **251F** (see Figure 1 for Chromatogram).

Compound	*m/z* (rel. int.)
235H[a] . . . . (scan 635)	235 (60), 234 (68), 220 (28), 206 (18), 178 (48), 165 (15), 164 (20), 152 (28), 150 (32), 138 (8), 136 (12), 112 (50), 111 (100), 98 (52), 96 (40).
245[a,b] . . . . (scan 775)	245 (20), 200 (10), 168 (12), 143 (5), 130 (8), 109 (100), 108 (55), 107 (60), 94 (30).
247[a] . . . . . (scan 758)	247 (50), 246 (24), 202 (7), 200 (9), 110 (38), 109 (100), 94 (12). high resolution: 247 (15), $C_{16}H_{25}NO$; 232 (2), $C_{15}H_{22}NO$; 202 (4), $C_{14}H_{20}N$; 200 (6), $C_{14}H_{18}N$; 110 (37), $C_{17}H_{12}N$; 109 (100), $C_7H_{11}N$.
247-Ac[a,b] . .	289 (8), 230 (13), 134 (6), 119 (10), 110 (100), 109 (80), 94 (12), 91 (22).
249B . . . . (scan 765)	249 (18), 248 (34), 222 (26), 221 (98), 220 (100), 206 (30), 192 (28), 186 (13), 178 (20), 172 (63), 168 (30), 166 (30), 164 (48), 152 (100), 136 (18), 124 (15), 114 (53), 111 (66), 98 (30), 96 (22), 82 (28), 69 (20).
251F . . . . (scan 816)	see Table 1.
251F-Ac[b] . .	294 (100), 293 (63), 292 (75), 278 (18), 264 (10), 250 (30), 237 (23), 236 (30), 235 (10), 234 (30), 220 (100), 178 (10), 162 (10), 152 (23), 150 (20), 112 (82), 111 (100), 96 (30), 82 (23).
251F' . . . . (scan 800)	251 (78), 250 (86), 236 (23), 222 (33), 221 (33), 220 (78), 195 (20), 194 (65), 180 (12), 165 (14), 164 (20), 152 (23), 150 (13), 112 (45), 111 (100), 98 (35), 96 (22), 82 (10), 81 (16), 79 (18), 68 (10).
251J . . . . . (scan 739)	251 (92), 250 (86), 236 (24), 234 (63), 222 (23), 208 (11), 195 (23), 194 (23), 178 (27), 164 (28), 152 (100), 150 (85), 138 (12), 124 (17), 112 (38), 111 (82), 98 (42), 96 (16), 82 (19), 69 (22).
265B . . . . (scan 879)	265 (80), 264 (100), 250 (35), 236 (45), 235 (50), 234 (82), 222 (12), 215 (12), 208 (12), 206 (15), 195 (20), 194 (50), 178 (18), 166 (22), 135 (15), 126 (30), 125 (50), 112 (20), 96 (26), 83 (10), 82 (10).
279B . . . . (scan 936)	279 (85), 278 (100), 264 (40), 254 (10), 250 (45), 249 (45), 248 (100), 236 (28), 233 (40), 222 (20), 210 (50), 194 (58), 180 (35), 164 (15), 139 (40), 126 (15), 117 (42), 110 (15), 98 (10), 96 (10), 82 (15).
279C . . . . (scan 871)	279 (100), 278 (95), 264 (43), 262 (64), 250 (21), 243 (23), 236 (23), 222 (22), 210 (8), 195 (22), 180 (64), 140 (23), 139 (33), 126 (28), 96 (13), 83 (12), 82 (10).

[a]Detected in fractions obtained during chromatography of **251F**. Scan times are from Figure 1 chromatogram.

[b]Mass spectra measured with Finnigan model 800 ion-trap.

ir data, combined with the ms-ms data and compatible cleavage mechanisms (Figure 5), led us to the cyclopenta[*b*]-quinolizidine structure **1** for **251F**.

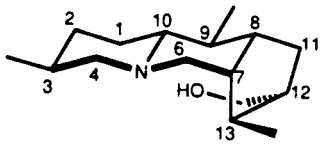

1 251F

The two-proton eight-line signal at δ 3.55 and 3.38 is recognized as an AB part of an ABX system [$J_{AB} = 11, J_{AX}$ (calcd) = 6.5, J_{BX} (calcd) = 5.5 Hz] and is assigned to the CH_2OH protons. Decoupling of these protons indicates the X proton (H-12) as a complex multiplet at δ 1.60. The five signals between δ 3.35 and 2.40 ppm, each corresponding to one proton, are assigned to hydrogens adjacent to a protonated nitrogen: H_{eq}-6 and H_{ax}-6 at δ 3.31 (d, J = 13.4 Hz) and δ 3.09 (dd, J = 13.4, 4.5 Hz), respectively; H_{eq}-4 and H_{ax}-4 at δ 3.18 (ddd, J = 12.2, 3.7, 2.2 Hz) and δ 2.49 (t, J = 12.4

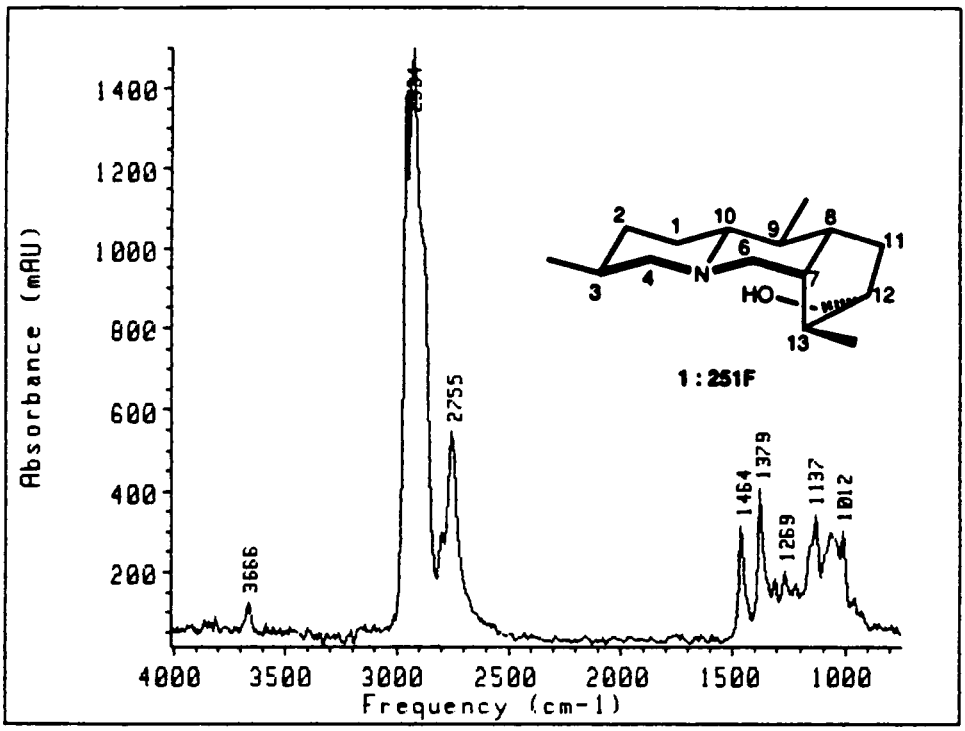

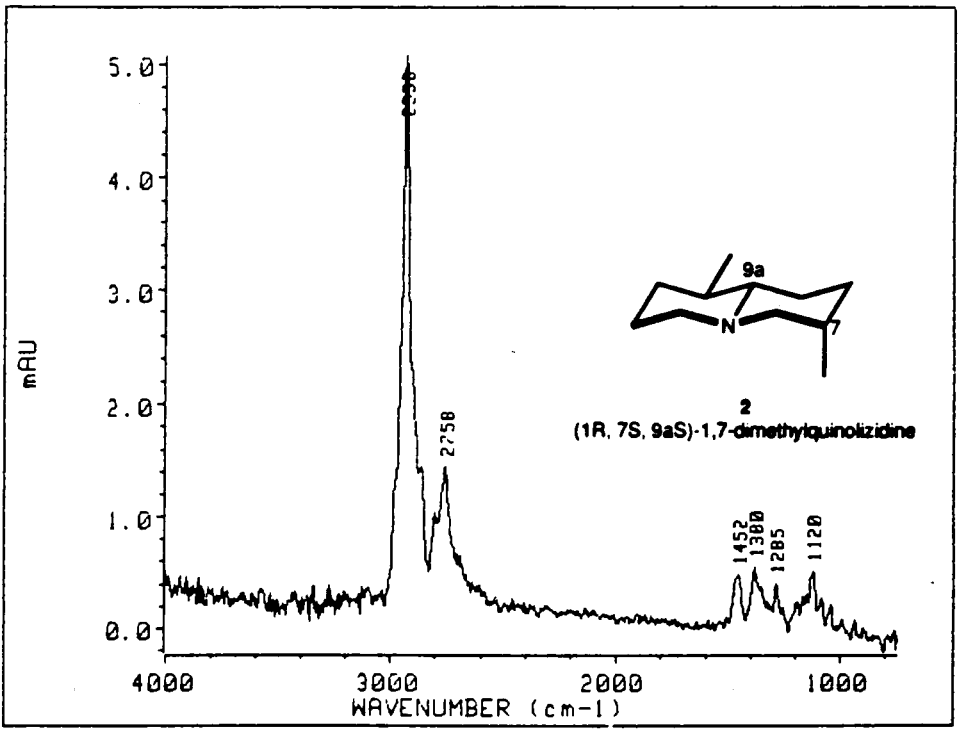

FIGURE 3. Gc-Ft-ir spectra of (a) alkaloid **251F** [**1**] and (b) 1,7-dimethylquinolizidine [**2**].

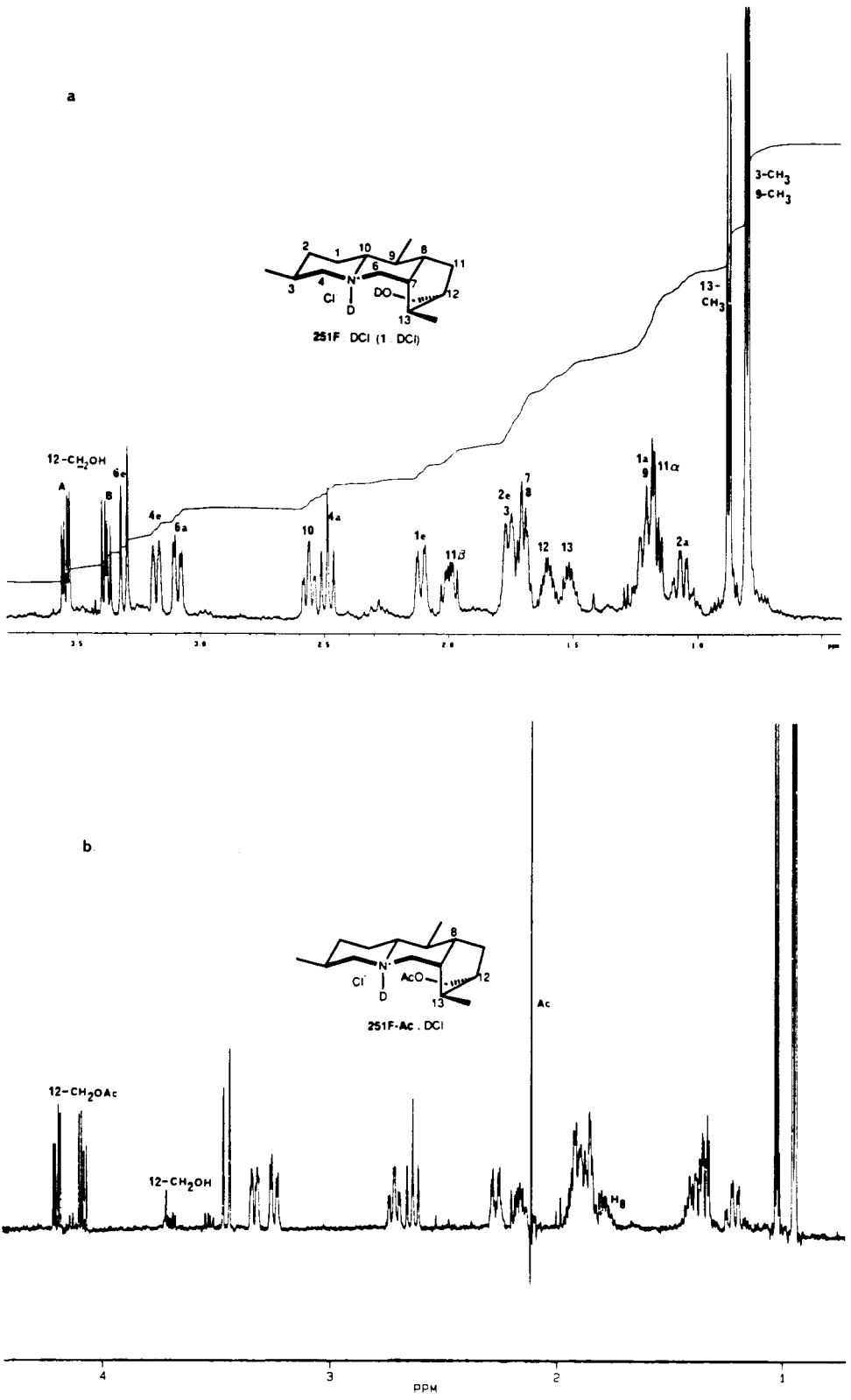

FIGURE 4. ^{1}H-nmr spectra (500 MHz, D_2O) of (**a**) alkaloid **251F** [**1**]·DCl (**b**) **251F**-Ac·DCl.

TABLE 3. ^{1}H-nmr Patameters for **251F** [**1**·DCl] (D_2O, 300 MHz).[a]

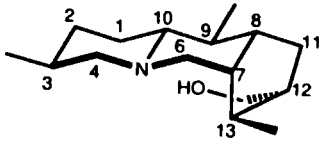

(see Figure 4a for proton integration)

Proton	δ (ppm)	Multiplicity	*J* (Hz)	Irradiation at		
				proton	affects	removes
H_{eq}-1	2.11	dq	14.6, 3.1–3.7	H_{eq}-1 (low power)	H_{ax}-1, H_{eq}-2	
					H_{ax}-2	small *J*→q
					H-10	small *J*→t
H_{ax}-1	1.24	m		H_{ax}-1	H_{eq}-1	large *J*
H_{eq}-2	1.75	m				
H_{ax}-2	1.06	qd	13.4,3.6			
H-3	1.75	m				
H_{eq}-4	3.18	ddd	12.2,3.7,2.2	H_{eq}-4	H-3	
					H_{ax}-4	large *J*→d
H_{ax}-4	2.49	t	12.4	H_{ax}-4	H_{eq}-4	large *J*→s
H_{eq}-6	3.31	d	13.4			
H_{ax}-6	3.09	dd	13.4,4.5	H_{ax}-6	H_{eq}-6	large *J*→s
					H-7	
H-7	1.72	m		H-7	H-11β	medium *J*→dd (14,11)
H-8[b]				H-8	H-13	
H-9	1.24	m				
H-10	2.56	td	11.3,3.1	H-10	H_{ax}-1, H-9[c]	
					H_{eq}-1	
H-11α	1.18	m		H-11α	H-1e,2a,10[d]	
					H-8	
					H-11β	large *J*→dd (11,8)
					H-12	small *J*

TABLE 3. (Continued)

Proton	δ (ppm)	Multiplicity	*J* (Hz)	Irradiation at		
				proton	affects	removes
H-11β	2.00	ddd	14.0, 10.7, 7.8	H-11β	H-8, -12	
					H-11α	large *J*
H-12	1.60	m		H-12	H-11α	small *J*
					H-11β	large *J*↦dd (14,8)
				H-12 (low power)	H-11α, -11β, -13	
H-13	1.52	m		H-13 (low power)	H-7, -12	
CH_2OH	3.55 (A)	dd	J_{AB} = 11.0;			
	3.38 (B)	dd	calcd J_{AX} = 6.5	H-A	H-12	medium *J*
					H-B	large *J*↦d
			calcd J_{BX} = 5.5	H-B	H-12[c]	
					H-A	large *J*↦d
3-Me (e)	0.80	d	6.4	3-Me	H-3, -9	
9-Me (e)				9-Me		
				H-9	9-Me	*J* = 6.4↦s
13-Me	0.88	d	6.4	13-Me	H-13	small *J*↦dd (11,10)

[a] 0.34 mg **251F** in D_2O containing 5 μmol DCl. Amount determined at end of experiment by addition of known amount of dioxane.
[b] δ 1.63 ddd ($J_{est.} \cong$ 12, 10, 7 Hz) in **251F**-Ac·DCl (see Figure 4b).
[c] Slash used to indicate overlapping signals.
[d] Protons 1e, 2a, and 10 also are affected due to irradiation of adjacent 1a/9.
[e] Small effect.
[f] 3-Me unaffected.

TABLE 4. Observed Connectivities in **251F [1]** as Determined with the RELAYH Method.[a]

^{1}H Signal	Relay = 0 (COSY)	Relay = 1	Relay = 2
H_{eq}-1	H_{eq}-2/H-3, H_{ax}-1/H-9, H_{ax}-2, H-10		9-Me
H_{ax}-1/H-9	H_{eq}-1, H_{eq}-2/H-3, H_{ax}-2, H-7/H-8, H-10, 3-Me/9-Me		
H_{ax}-2	H_{eq}-1, H_{eq}-2/H-3, H_{ax}-1/H-9	H_{ax}-4, H-10, 3-Me/9-Me	H_{eq}-4
H_{eq}-2/H-3	H_{eq}-1, H_{ax}-1/H-9, H_{ax}-2, H_{eq}-4, H_{ax}-4, 3-Me/9-Me		
H-3 (see above)	H_{eq}-4, H_{ax}-4, 3-Me/9-Me		
H_{eq}-4	H_{ax}-4, H_{eq}-2/H-3	3-Me	H_{ax}-2
H_{ax}-4	H_{eq}-4, H_{eq}-2/H-3	H_{ax}-2	
H_{eq}-6	H_{ax}-6		
H_{ax}-6	H_{eq}-6, H-7/H-8		13-Me
H-7/H-8	H_{ax}-6, H-11α, H-11β, H-13	H_{eq}-6, H-10, 13-Me	
H-8 (see above)	H-11α, H-11β, 3-Me/9-Me	H-10	
H-9 (see above)	H-7/H-8, H-10, 3-Me/9-Me		
H-10	H_{eq}-1, H_{ax}-1/H-9	H-7/H-8, 9-Me	
H-11α	H-11β, H-12	CH_2OH (A,B)	13-Me
H-11β	H-7/H-8, H-11α, H-12	CH_2OH (B)	9-Me
H-13	H-7/H-8, 13-Me		
CH_2OH (A)	H-12	H-11α	13-Me
CH_2OH (B)	H-12	H-11α, H-11β	13-Me
3-Me—9-Me	H_{ax}-1/H-9, H_{eq}-2/H-3	H_{ax}-2, H_{eq}-4, H_{ax}-4, H-10	H_{eq}-1, H-11β
9-Me/3-Me (see above)	H_{ax}-1/H-9	H-10	H-11β
13-Me	H-13	H-7/H-8	H_{ax}-6, H-11α, CH_2OH (A,B)

[a]For overlapping signals as indicated by a slash, we propose the inferred, most likely couplings by underlining.

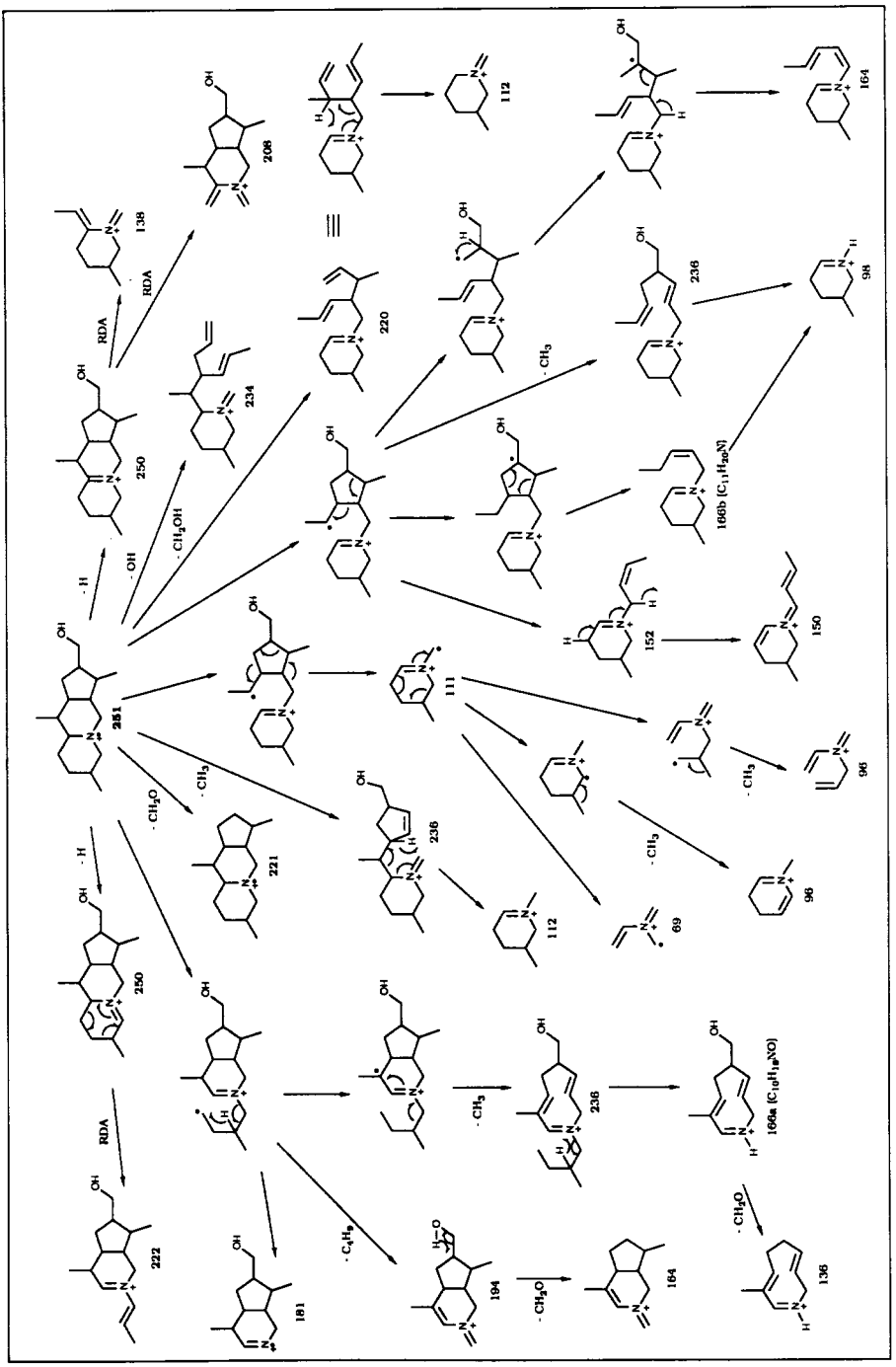

FIGURE 5. Cleavage pathways proposed for alkaloid **251F** (all ions shown are of intensity ≥ 10%).

Hz), respectively, and H-10 as a triplet of doublets at δ 2.56 (J = 11.3, 2.1 Hz). Moynehan *et al.* (8) report a range of δ 3.4–3.0 for these protons in various protonated Me quinolizidinium salts in $CDCl_3$. The signal for H_{eq}-4 can be explained by invoking a long range W-coupling with H_{eq}-2, in addition to the geminal and vicinal, $J_{4e,3a}$, coupling. Martin *et al.* (9) report a similar long-range coupling ($J_{6e,8e}$) of 2.0 Hz in a quinolizidine. The absence of spin coupling between H_{eq}-6 and H-7 ($J < 1$ Hz) indicates that the H_{eq}-6–H-7 dihedral angle is close to 90°, presumably resulting from the effect of a cyclopentane ring cis-fused to C-7 and C-8 of the quinolizidine ring. A computer energy minimization program, Quanta Molecular Modelling Program version 3.0, yielded a value of 65° for this angle (Table 5), resulting in a J of less than 2 Hz.

TABLE 5. Calculated Dihedral Angles for Selected Vicinal Hydrogens Involving the **251F** Cyclopentane Ring.[a]

Vicinal Hydrogens	Dihedral Angle (°)	Observed J (Hz)
H-7, H_{eq}-6	65	< 1
H-7, H_{ax}-6	51	4.4
H-7, -8	44	—[b]
H-7, -13	164	11.2
H-8, -9	167	—[b]
H-8, -11α	88	0
H-8, -11β	30	8
H-9, -10	175	11.3
H-12, -11α	105	6.8
H-12, -11β	11	11
H-12, -13	141	10.2

[a]Computer program used was Quanta Molecular Modelling Program, Version 3.0, on a Silicon Graphics RS 40 computer and IRIS 40 work station.

[b]Chemical shifts of these vicinal hydrogens are very close and J values could not be observed.

Slight distortions of the cyclopentyl ring cause significant changes in the H_{eq}-6–H-7 dihedral angle. The one-proton signal at δ 2.11 appears as a doublet of quartets (J = 14.6, 3.1–3.7 Hz) and is assigned to H_{eq}-1 since it is coupled to H-10 with a small J (decoupling experiment). It is also coupled with a small J to the upfield quartet of doublets at δ 1.06, a signal assigned to H_{ax}-2 ($J_{2a,2e} \cong J_{2a,3a} \cong J_{1a,2a} \cong 13.4$, $J_{1e,2a} \cong$ 3.6 Hz). The δ 2.00 signal (8 lines, ddd) is assigned to H-11β, downfield relative to the H-11α due to the shielding effect of the neighboring hydroxymethyl group upon H-11α (10). Two one-proton multiplets are seen at δ 1.60 and 1.52 and are assigned by decoupling experiments to the X-proton (H-12) of the ABX system (discussed earlier) and the proton (H-13) coupled with the downfield 13-Me at δ 0.88, respectively. The H-13 signal appears as 12 lines with J values of 12.2, 10, and 6.2 Hz being discernable. Calculated dihedral angles for H-11β with H-8 and H-12 are 30° and 11°, respectively, in agreement with measured J values for H-11β (7.8, 10.7, 14.0 Hz) indicating one medium and one large vicinal coupling, in addition to the geminal (14 Hz) coupling. Irradiation of the H-7/H-8 signal removes the 7.8 Hz coupling from H-11β, while irradiation of H-12 removes the 10.7 Hz coupling from H-11β and a 6.8 Hz coupling from the H-11α signal at δ 1.49 (Table 3).

Because of the broadness of the H-12 and H-13 signals, a cross peak indicating scalar coupling is missing in the H-COSY spectrum. Nevertheless, in RELAYH experiments (Table 4) we can see connectivity between the CH_2OH protons and 13-Me

(relay = 2) and connectivity between the CH_2OH group and both H-11α and H-11β (relay = 1). Irradiation of the 13-Me signal collapses the δ 1.52 multiplet assigned to H-13 to a simple triplet-like doublet of doublets (J = 10.2, 11.2 Hz) greatly skewed by coupling to the adjacent downfield H-12 signal.

The H-COSY, RELAYH, and decoupling experiments locate the remaining protons as indicated in Figure 4a. Two of the axial protons (H_{ax}-1, H-9) are found under the δ 1.2 envelope along with the H-11α, while the other two axial protons (H-3, H-8) are located with the remaining two equatorial hydrogens (H_{eq}-2, H-7) under the δ 1.68–1.78 multiplet.

A sample of **251F** was acetylated to the CH_2OAc derivative and the ^{1}H-nmr spectrum measured as the deuterochloride in D_2O (Figure 4b). Little new information was obtained. However, both H-12 and H-13 have undergone downfield shifts and now lie under the δ 1.82–1.95 envelope, while a new one-proton signal assigned to H-8 has emerged upfield of this complex pattern. This signal is composed of three overlapping doublets with estimated J values of 7, 10, and 12 Hz, assigned to $J_{8,11\beta}$, $J_{7,8}$, and $J_{8,9}$, respectively ($J_{8,11\alpha} \cong 0$). As would be expected, the CH_2OAc signals are significantly shifted downfield. Note, however, that the Me pattern has not changed, and also that signals (CH_2OH, 13-Me) due to small amounts of **1** produced by partial hydrolysis of **251F**-Ac can be seen.

Three Me's are indicated, one at δ 0.88 (J = 6.4 Hz) and two overlapping at δ 0.80 (J = 6.4 Hz). The H-COSY spectrum ruled out either $CH(Me)_2$ or $CH(Me)CH_2OH$ moieties, indicating that all three Me's must be ring substituents. We have assigned to the two upfield Me's equatorial configurations at C-3 and C-9 in order to accommodate the proton coupling data for H_{eq}-4, H_{ax}-4, and H-10. The H-COSY and RELAYH experiments confirmed Me's at C-3 and C-9 and located the third at C-13 (Table 4).

The usual δ_{eq}-δ_{ax} value for quinolizidine C-4 and C-6 hydrogens [0.8, cf. Crabb (11)] is seen for H_{eq}-4–H_{ax}-4 where they are similarly shielded by the 3-Me_{eq} group, while the smaller separation for H_{eq}-6–H_{ax}-6 (0.2) may be a consequence of H_{eq}-6, but not H_{ax}-6, being shielded by the bulky axial substituent at C-7. Note that 1,7-dimethylquinolizidine [**2**, see Figure 3b] has a δ_{4e}–δ_{4a} of 0.84 and a δ_{6e}–δ_{6a} of 0.40, where the axial 7-Me group has a similar effect in reducing the separation for the C-6 hydrogens (7).

An H-NOESY spectrum exhibited significant cross peaks, indicating nOe's for the five β-axial hydrogens (2a-4a; 4a-10; 2a-10; 4a-6a; 6a-10; 4a-10; 6a-8; 8-10; 6a-10), two α-axial hydrogens (1a-3) and interactions consistent with the presence of Me groups at C-3, C-9, and C-13, viz., nOe's between 3-Me with three protons H_{ax}-2, H_{eq}-4, and H_{ax}-4; 9-Me with H_{eq}-1; H-7/H-8 with H-10 and H-11α and lastly both 13-Me (strong) and H-13 (weak) with H_{eq}-6. A strong cross peak between H_{eq}-4 and H_{eq}-6 is also detected. Note that the cross peak expected for H_{ax}-1 and H-9 is not seen because those signals overlap. The data are consistent only with a trans quinolizidine with equatorial Me's at C-3 and C-9 and an axial bulky group at C-7.

The stereochemistry of the 13-Me and CH_2OH groups in the cyclopentane ring, while not as unambiguously fixed by the NOESY data as would be the case for adjacent groups in a cyclohexane ring, is nevertheless most consistent with an H-12–H-13 trans configuration and a β-oriented 13-Me group. The following strong cross peaks are observed: H-13 with CH_2OH (both A and B); 13-Me with H-12; H-7/H-8 with H-12; H-11α with CH_2OH (A,B) (no H-11β with CH_2OH); H-9 with H-13; and H-7 with 13-Me, which fit only the trans configuration shown. One pair of weak interactions [13-Me with CH_2OH (A and B)] is also seen.

This structure seemed at first difficult to reconcile with the observation of two large (10.2, 11.2 Hz) couplings detected between H-13 and H-7 and H-13 with H-12,

when the 13-Me is decoupled, and also again, two large J values (10.3, 10.2 Hz) observed for H-12 with H-13 and H-11β when the more strongly coupled hydrogen (A) of the CH_2OH signal is decoupled. A computer model for structure **1** after energy minimization yielded the calculated dihedral angles of Table 5, where it is seen that both the H-7–H-13 and H-13–H-12 dihedral angles (164°, 141°) are significantly larger than the usual 120° expected for a cyclopentane ring and would be expected to yield larger coupling constants. It has been noted that vicinal hydrogens in furanose derivatives with dihedral angles greater than 150° have $J_{trans} \geq J_{cis}$ (12).

The ^{13}C-nmr spectrum of **1** (see Experimental) exhibits the expected sixteen signals with no vinyl or quaternary carbons. A reverse detection HMQC spectrum allows the assignment of most of the carbon signals with uncertainties only for the 3-Me/9-Me and C-7/C-8 pairs. The C-6 signal at 53.2 ppm may indicate a γ effect is operative involving the 13-Me substituent. All our ^{13}C assignments are compatible with data reported for quinolizidines (13) and *trans*-2-methylcyclopentylmethanol (14).

The major fragmentation pathways, which we propose to accommodate the eims data and the ms-ms experiments, are shown in Figure 5. Note particularly that the pathway producing the pair of ions at *m/z* 152 and 150, arising from $[M-C_6H_{11}O]^+$ and $[M-C_6H_{13}O]^+$, is responsible for locating the hydroxymethyl group at C-12 and one Me at C-13, but not at C-11. In some pathways the loss of CH_2O is concerted with other bond ruptures; in some (e.g. 194↦164), it is not.

Alkaloid **251F** is accompanied by at least nine congeners, all having significant (if not base) peaks at odd mass (e.g., *m/z* 109, 125, 139, etc). One (**235H**) is a deoxy-**251F**, while another (**247**) is a didehydro-**251F**. The latter showed a strong ir absorption at 1692 cm^{-1} on gc-Ft-ir (enamine $\nu_{c=c}$), had an exchangeable hydrogen, and gave a monoacetate, which showed a strong acetoxy loss ($[M-59]^+$ but no $[M-CH_2OAc]^+$) on gc-ms, typical of an allylic acetate (see Experimental). The mass measured formula for the molecular ion was $C_{16}H_{25}NO$ and for the *m/z* 109 fragment was $C_7H_{11}N$. Another congener, **249B**, appears to be an aldeyde, showing a loss of 29 amu (CH=O) in its eims rather than the 31 amu loss for **251F**. A **251F** homologue, **265B**, and a bis homologue, **279B**, also have a CH_2OH group. One isomer each of **251F** and **279B** lack this 31 amu loss but instead show a major loss of 17 amu (OH), suggesting tentative structures **251J** and **279C** with tertiary rather than primary hydroxyls. The **251F** base peak of *m/z* 111 is replaced by a weaker *m/z* 125 peak in the homologue **265B** and *m/z* 139 in both bis homologues **279B** and **279C**. A more significant Me or Et loss, respectively, is seen in **265B** and both **279B** and **279C**. Another isomer, **251F′**, is seen, which appears to be a primary alcohol and is probably a diastereomer of **251F**. Finally, a trace alkaloid **245** is seen, which has an *m/z* 109 base peak similar to that of **247**.

The loss of 57 amu, yielding a major fragment *m/z* 194 for **251F**, is still seen in the two isomers **251F′** and **251J**, in **249B** (*m/z* 192), weakly in the bis homologues **279B** and **279C** (*m/z* 222), and very weakly in the homologue **265B** (*m/z* 208). In the latter case, the presence of *m/z* 194 may indicate that a 71 amu loss now replaces the 57 amu loss. The *m/z* 152 fragment of **251F**, corresponding to $[M-C_6H_{11}O]^+$, is probably replaced by a fragment at *m/z* 166 in **265B** and one at *m/z* 180 in the bis homologues **279B** and **279C**. The cleavage pathway yielding the *m/z* 152 or 180 fragment is enhanced in **249** and the putative tertiary alcohols **251J** and **279C**.

We suspect all these congeners share the same carbon skeleton and probably have the same stereo configuration for most substituents. However, without further supplies for additional structural work we can propose only tentative structures for them (Figure 6). These structures may devolve from a common sesquiterpenoid moiety formed from the usual head-to-tail linkage of two isoprenes with a third isoprene joined at internal

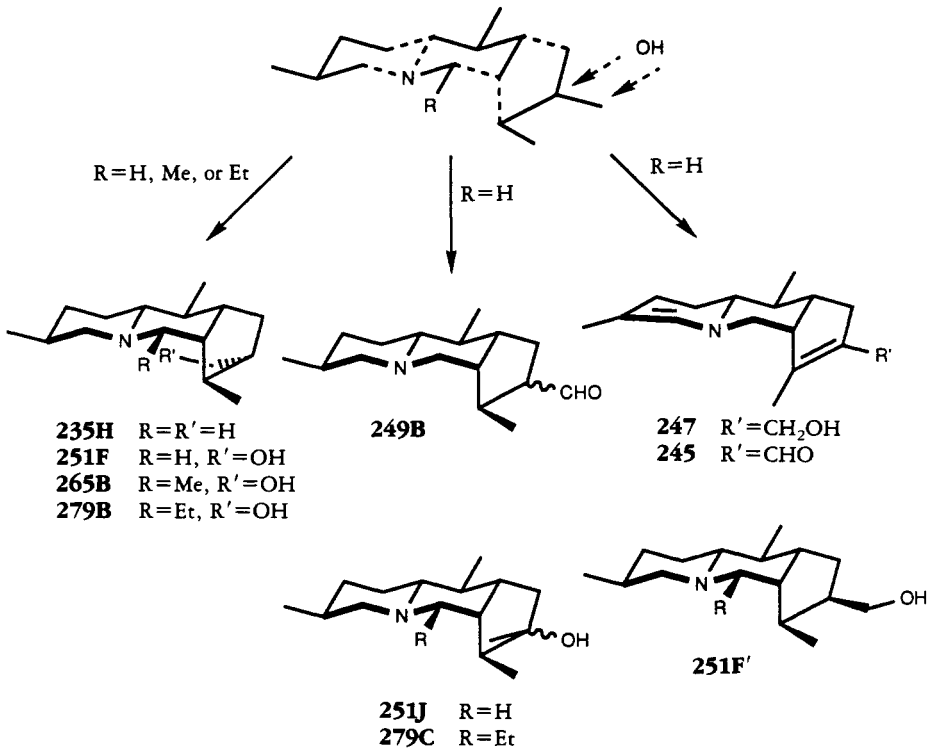

FIGURE 6. Alkaloid **251F** and tentative structures and possible isoprenoid origins of cyclopenta[*b*]quinolizidines of the poison frog *Minyobates bombetes*.

and head positions. This sesquiterpenoid and an alkylamine could be condensed (no actual sequence of steps is implied) to generate **251F** and its congeners.

EXPERIMENTAL

GENERAL EXPERIMENTAL PROCEDURES.—A Finnigan 4500 mass spectrometer or a Finnigan model 800 ion-trap mass detector interfaced with a Hitachi gas chromatograph were used for gc-ms studies. The former was fitted with a 25 m × 0.25 mm OV-1 fused silica bonded column; the latter with a 30 m × 0.20 mm HP-5 (Hewlett-Packard 5% polyphenylmethylsiloxane: 95% polydimethylsiloxane) fused silica bonded column. Cims with the Finnigan 4500 used NH_3, ND_3 or isobutane as reagent gases. A Finnigan TSP46 mass spectrometer with direct injection was used for ci thermospray ms. Deuterated buffers (60% D_2O/MeCN containing 0.05 M NH_4OAc) permitted the quantitation of exchangeable hydrogens. Hrms for **247** used a JEOL SX102 instrument fitted with a 15 m × 0.20 mm HP-5 column. Ms-ms studies used a Finnigan ion-trap mass spectrometer (ITMS) (15). ^{1}H-nmr spectra in D_2O were measured with either Varian XL-300 or Varian VXR-500S spectrometers. Chemical shifts (δ, ppm) are referred to HOD at δ 4.78. ^{13}C-nmr, ^{1}H 2D-COSY and ^{1}H reverse detection HMQC experiments were carried out on the Varian VXR-500S spectrometer.

Gc-Ft-ir spectra were obtained using a Hewlett-Packard model 5965A instrument with a narrow band (4000–750 cm^{-1}) detector and a 59970 IRD ChemStation interfaced with a Hewlett-Packard model 5890 gas chromatograph having an HP-5 capillary column (30 m × 0.32 mm) and program similar to those used with the Finnigan model 800 ion-tap.

BIOLOGICAL MATERIAL AND EXTRACTION.—An alkaloid fraction was prepared from MeOH extracts of skins of the poison frog *M. bombetes* (100 skins, 6 g wet wt) from Lago Calima, Departamento Valle, Colombia, by solvent partitions as described (6). Voucher specimens are located in the American Museum of Natural History, New York. Evaporation of a major portion of the alkaloid fraction gave a residue of 2.7 mg, which was chromatographed on a silica gel column (0.2 g, Merck 60). Using CH_2Cl_2 and 2–8% MeOH/CH_2Cl_2, 47 fractions of 1 ml each were collected and analyzed with gc-ms (ion trap) and thermospray (direct injection) ms, the latter with 60% H_2O/MeCN or 60% D_2O/MeCN buffers contain-

ing 0.05 M NH_4OAc to provide $[M + H]^+$ or $[M + D]^+$ peaks for each alkaloid component present. Alkaloid **251F** appeared in fractions 22–41 (0.34 mg), and these fractions were used for nmr and other studies.

Hydrogenation with 5% Rh/Al_2O_3 or PtO_2 in MeOH (100 µl of original solution) at 2 atm H_2 was performed using an electrolytic hydrogen generator, followed by analysis by gc-ms.

Acetylation was performed with freshly distilled Ac_2O at room temperature for 24 h, followed by removal of excess Ac_2O with a stream of N_2. One chromatographic fraction containing **247** was also acetylated. The acetylated **251F** was purified by silica gel cc as described above for **251F**. For ms data see Tables 1 and 2. ^{13}C nmr δ_c (ppm) for **251F**·DCl (in D_2O) (nt, 188,000) (assignments by reverse detection HMQC) 14.77 (13-Me), 15.67 (9-Me)*, 17.54 (3-Me)*, 27.14 (1), 28.40 (3), 30.23 (2), 31.43 (11), 35.41 (13), 37.67 (9), 41.26 (7)$^+$, 44.37 (8)$^+$, 47.36 (12), 53.19 (6), 61.38 (4), 64.84 (CH_2OH), 67.40 (10) (*,$^+$ assignments within each pair could be reversed).

ACKNOWLEDGMENTS

We thank Dr. F.W. Fowler, Department of Chemistry, State University of New York, Stony Brook, New York, for a generous sample of 1,7-dimethylquinolizidine, which was so useful to our studies. We are indebted to Dr. F. Carlos Lehmann Valencia, the late director of the Museo de Ciencias Naturales (Cali), who facilitated our (J.W.D.) field work in Colombia.

LITERATURE CITED

1. J.W. Daly, C.W. Myers, and N. Whitaker, *Toxicon*, **25**, 1023 (1987).
2. J.W. Daly, R.J. Highet, and C.W. Myers, *Toxicon*, **22**, 905 (1984).
3. J.W. Daly, H.M. Garraffo, L.K. Pannell, T.F. Spande, C. Severini, and V. Erspamer, *J. Nat. Prod.*, **53**, 407 (1990).
4. J.W. Daly, G.B. Brown, M. Mensah-Dwumah, and C.W. Myers, *Toxicon*, **16**, 163 (1978).
5. C.W. Myers, *Pap. Avulsos Dep. Zool. Secr. Agric. Ind. Comer. (Sao Paulo)*, **36**, 301 (1987).
6. C.W. Myers and J.W. Daly, *Am. Mus. Novit.*, No. 2692, 1 (1980).
7. Y.C. Hwang and F.W. Fowler, *J. Org. Chem.*, **50**, 2719 (1985).
8. T.M. Moynehan, K. Schofield, R.A.Y. Jones, and A.R. Katritzky, *J. Chem. Soc.*, 2637 (1962).
9. T.I. Martin, D.B. MacLean, J.T. Wróbel, A. Iwanow, and W. Starzec, *Can. J. Chem.*, **52**, 2705 (1974).
10. E. Pretsch, H. Immer, C. Pascual, K. Schaffner, and W. Simon, *Helv. Chim. Acta*, **50**, 105 (1967).
11. T.A. Crabb, *Annu. Rep. NMR Spectrosc.*, **6A**, 323 (1975).
12. R.V. Lemieux and J.W. Lown, *Can. J. Chem.*, **41**, 889 (1963).
13. F. Bohlmann and R. Zeisburg, *Chem. Ber.*, **108**, 1043 (1975).
14. H.C. Brown, R.G. Naik, R.K. Bakshi, C. Pyun, and B. Singaram, *J. Org. Chem.*, **50**, 5586 (1986).
15. L.K. Pannell, Q.-L. Pu, R.T. Mason, and H.M. Fales, *Rapid Commun. Mass Spectrom.*, **4**, 103 (1990).

Received 25 July 1991